Carbohydrate Polymers 74 (2008) 666–672

Contents lists available at ScienceDirect

Carbohydrate Polymers

journal homepage: www.elsevier.com/locate/carbpol

Biofunctionality of self-assembled nanolayers composed of cellulosic polymers

Shingo Yokota *, Takuya Kitaoka, Hiroyuki Wariishi

Department of Forest and Forest Products Sciences, Graduate School of Bioresource and Bioenvironmental Sciences, Kyushu University, 6-10-1 Hakozaki, Higashi-ku, Fukuoka 812-8581, Japan

ARTICLE INFO

Article history:
Received 3 March 2008
Received in revised form 11 April 2008
Accepted 15 April 2008
Available online 25 April 2008

Keywords:
Cellulosic polymer
Biointerface
Surface morphology
Cell attachment
Self-assembly

ABSTRACT

Biofunctional cellulosic interfaces were successfully designed via the self-assembly of cellulose and its derivatives whose reducing ends were selectively modified with thiosemicarbazide. The biological functions of cellulosic self-assembled monolayers (SAMs) formed on a gold surface were investigated using rat liver cells. The cells proliferated well on the cellulose SAM (cellulose I) and methylcellulose SAM, while almost no cells adhered to the regenerated cellulose film (cellulose II) and hydroxyethylcellulose SAM. In the initial cell adhesion, rat liver cells were moderately attached on the cellulose SAM even in serum-free culture, possibly suggesting specific interactions between cells and cellulose SAM with unique surface morphology. The architectural design of cellulosic nanolayers via peculiar vectorial chain immobilization is expected to provide new information for the functional development of structural polysaccharide-based biointerfaces.

1. Introduction

The extracellular matrix plays a fundamental role in regulating various cellular processes involved in proliferation, migration, differentiation, and survival. To date, many scaffold materials for cell and tissue engineering have been reported with a view to stimulating cell adhesion and specific cellular functions (Boyan, Hummert, Dean, & Schwartz, 1996; Lim, Liu, Vogler, & Donahue, 2004; Park et al., 2003). It is well known that cells sense and respond to signals from biomaterial surfaces depending on their chemistry, topography, charge, and wettability. To understand the cell response mechanism and develop biofunctional material, many researchers have made efforts to control the surface morphology on the order of nano and micrometers of materials designed from a variety of resources including metals, ceramics, polymers, and composites (Couet, Rajan, & Mantovani, 2007; Du et al., 2006; Jagur-Grodzinski, 2006; Lim et al., 2007; Nakanishi et al., 2006). In particular, polymers are recognized as fascinating resources of biomaterials owing to easy processability and functional diversity, resulting in numerous successful preparations of bioactive interfacial material composed of bioderived and synthetic polymers (Couet et al., 2007; Jagur-Grodzinski, 2006).

Cellulose, a linear polysaccharide consisting of D-glucose units repeated via β-1,4 linkages, is the major skeletal component in higher plants and an abundant, almost inexhaustible, biodegradable, and biocompatible polymer (Klemm, Heublein, Fink, & Bohn, 2005). As a raw material, cellulose can be converted to a diverse array of cellulose derivatives by chemical modifications (*e.g.* esterification and etherification) (Nishio, 2006). To date, cellulose and its derivatives have been extensively used in not only traditional papermaking and textile fiber industries, but also pharmaceutical and biomedical fields (Czaja, Young, Kawecki, & Brown, 2007; Hoenich, 2006; Klemm, Schumann, Udhardt, & Marsch, 2001; Klemm et al., 2005, 2006). One of the historical uses of cellulosic polymers in medicine is as a hemodialysis membrane mainly composed of regenerated cellulose or cellulose acetate because of its blood compatibility (Hoenich, 2006). In the evolving biomedical field, bacterial cellulose (BC, synthesized by *Acetobacter xylinum*) has recently attracted much attention as a promising cellulose-based biomaterial for wound dressings, artificial blood vessels, and scaffold material for tissue engineering (Czaja et al., 2007; Hoenich, 2006; Klemm et al., 2001, 2005, 2006). The unique nanostructure of BC, including its specific crystal structure, high crystallinity, and nanofiber network, offers high tensile strength, high water holding capacity, and excellent biocompatibility (Czaja et al., 2007; Hoenich, 2006; Klemm et al., 2001, 2005, 2006). In addition, chemical modification (*e.g.* phosphorylation and sulfation) of BC was actively investigated to improve the bioactivity of BC-based cell culture scaffolds (Bodin et al., 2007; Svensson et al., 2005). Thus, the nanostructure and/or chemical property of the surface layers of the cellulosic materials have a great impact on the function of cellulose-related biomaterials.

A cellulose molecule has inherently unique features for self-assembly and hierarchical organization via regular intra- and intermolecular hydrogen bond networks leading to specific crystal structures and polymorphs (Atalla & VanderHart, 1984; Nishiyama, Langan, & Chanzy, 2002; Nishiyama, Sugiyama, Chanzy, & Langan,

* Corresponding author. Tel./fax: +81 92 642 2995.
E-mail address: yokota@agr.kyushu-u.ac.jp (S. Yokota).

0144-8617/$ - see front matter © 2008 Elsevier Ltd. All rights reserved.
doi:10.1016/j.carbpol.2008.04.027

2003), which govern the characteristics of cellulosic materials. In nature, the cellulose molecules gather to form cellulose I-type crystal structures, with regularly packed, parallel-chain alignments along the longitudinal axis (Chanzy & Henrissat, 1985; Hieta, Kuga, & Usuda, 1984). However, the metastable cellulose I structure is usually converted to thermodynamically stable cellulose II through one-way transformation from parallel to anti-parallel alignment by mercerization and regeneration (Kolpak & Blackwell, 1976; Langan, Nishiyama, & Chanzy, 1999). In cellulose surface chemistry and physics fields, cellulose model films have been prepared by various methods (Kontturi, Tammelin, & Österberg, 2006). However, all the films adopt cellulose II structure with an anti-parallel arrangement or non-crystalline morphology, except a non-woven-like nanocrystal mat with cellulose I, although these surfaces have a slight problem with having sulfate groups attached on the cellulose crystals (Edgar & Gray, 2003). Thus, it is quite difficult to artificially control the cellulose chain alignments, in particular the surface layer state, resulting in few attempts to design a cellulosic material based on its chain alignment structure.

Recently, we designed a stable and pure cellulose nanolayer with cellulose I crystal structure on a gold surface from a cellulose solution, using terminal modification and self-assembly chemisorption techniques (Yokota, Kitaoka, Sugiyama, & Wariishi, 2007a). This novel cellulose self-assembled monolayer (SAM) can act as a model crystal surface with cellulose I structure, which provides information on the effect of chain alignment and crystal structure on a variety of properties of cellulosic material surfaces. Furthermore, the preparation protocol of a cellulose SAM was successfully applied to several water-soluble cellulose derivatives like methylcellulose (MC) (Yokota, Matsuyama, Kitaoka, & Wariishi, 2007b), which is expected to facilitate the wide design of functional cellulosic materials using various cellulose derivatives. In the present study, an adhesive animal cell was cultured on the resultant cellulosic nanolayers to investigate their surface functions from a biological point of view. In particular, an assay for cell adhesion, which is one of the most fundamental cellular responses to culturing materials, was performed. The relationships between aspects of the surface morphology, including chemical composition and the crystal structure of cellulosic nanolayers, and cell adhesion and proliferation, are discussed.

2. Materials and methods

2.1. Materials

Cellulose polymer (degree of polymerization (DP): *ca.* 200 (Cel_{200})) and oligomer (DP: *ca.* 6 (Cel_6)) were obtained from cotton cellulose powder (CF1, Whatman International Ltd., UK) by mercerization with 4 M sodium hydroxide solution (Schenzel & Fischer, 2001), and hydrolysis with phosphoric acid (Isogai & Usuda, 1991), respectively. MC (degree of substitution (DS): *ca.* 1.8; molecular weight (M_W): *ca.* 3×10^4 g mol^{-1}); and hydroxyethylcellulose (HEC, hydroxyethyl molar substitution (MS): *ca.* 1.5; M_W: *ca.* 5×10^5 g mol^{-1}) were purchased from Wako Pure Chemical Industries, Ltd. (Japan). *N*-Methylmorpholine-*N*-oxide (NMMO) and thiosemicarbazide (TSC) were obtained from Sigma–Aldrich Corp. and Wako (Japan), respectively. Polyvinylamine (PVAm, M_w: *ca.* 1×10^6 g mol^{-1}; charge density: 3.8 meq g^{-1}) was prepared by the partial hydrolysis of synthesized polyvinylformamide (Wang & Tanaka, 2000). Micro cover glass (diameter: 15 mm, Matsunami Glass Ind., Japan) was used as a flat and transparent substrate. The water used in this study was purified with a Milli-Q system (Millipore Inc.). A rat liver cell line (IAR-20) was provided by the Human Science Research Resources Bank (Japan). Eagle's minimum essential medium (EMEM), penicillin–streptomycin, trypsin, and ethylenediaminetetraacetic acid (EDTA) were obtained from Invitrogen Corp. Fetal bovine serum (FBS) and phosphate buffered saline (PBS) were purchased from Biowest Co. Ltd. (France) and Nissui Pharmaceutical Co. Ltd. (Japan), respectively. Tissue culture polystyrene (TCPS) dishes and plates (24-well) were obtained from Sumitomo Bakelite Co. Ltd. (Japan). Other chemical reagents were reagent grade and used without further purification.

2.2. Preparation of cellulosic nanolayers

TSC-labeling of cellulosic polymers and cellulosic SAMs (Fig. 1) were prepared essentially according to the method reported previously (Yokota et al., 2007a, 2007b). Cellulose samples (Cel_{200} and Cel_6, 1% (w/w)) were reacted with 1% (w/w) TSC in an 80% (w/w) NMMO/H_2O solution (65 °C, 90 min), and this was followed by precipitation of the resulting cellulose thiosemicarbazone (Cel_{200}- and Cel_6-TSC) with ethanol. The X-ray diffraction of Cel_{200}-TSC deposits showed the typical pattern of the cellulose II structure (Yokota et al., 2007a). The crude cellulose-TSCs were rinsed with ethanol by repeated centrifugation (at least three times). A piranha-washed glass plate was coated with gold (thickness: *ca.* 30 nm) using an ion sputter (VPS-020, ULVAC Inc., Japan). The gold-coated glass plate was soaked in 0.1% (w/w) Cel_{200}-TSC/NMMO solution (70 °C, 12 h). After soaking, the treated gold plate was thoroughly washed with 80% (w/w) NMMO solvent (105 °C, 30 min), and this followed by rinsing first with 50% (w/w) NMMO solution (r.t.,

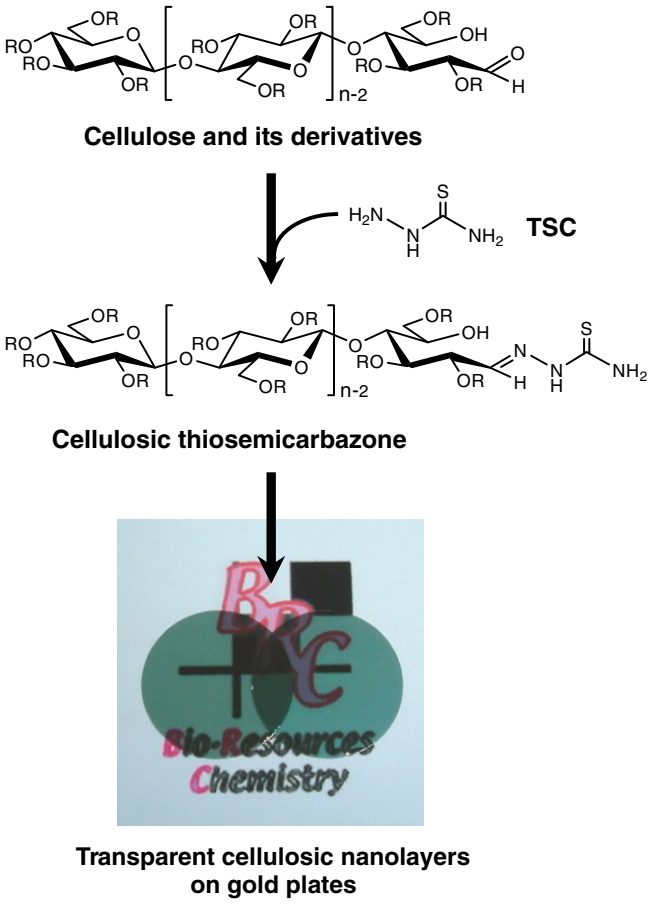

Fig. 1. Schematic illustration of the selective modification of cellulose and its derivatives with thiosemicarbazide (TSC) and a photograph of Cel_{200}-SAMs. R: H, cellulose; R: H or CH_3, methylcellulose; R: H or CH_2CH_2OR, hydroxyethylcellulose.

30 min) and then with deionized water (r.t., 4 h). In the case of Cel_6, the gold plate was soaked in 0.1% (w/v) Cel_6-TSC aqueous solution (r.t., 12 h) and then washed with deionized water (r.t., 4 h).

In clear 1% (w/v) aqueous MC and HEC solutions, an equivalent amount of TSC was added and heated while stirred (60 °C, 90 min), and this was followed by precipitation and repeated centrifugation (at least three times) of the MC- and HEC-TSCs with ethanol. Gold plates were immersed in 0.2% (w/v) MC- and HEC-TSC solutions of ethanol/water (1/2 v/v) at 4 °C for 12 h and then rinsed with deionized water (4 °C, 3 h) and methanol (r.t., 1 h).

Regenerated cellulose film (Cel_{200}-film) was prepared on a glass plate pretreated with PVAm by spin coating, basically according to previously reported protocol (Yokota, Kitaoka, & Wariishi, 2007c). Cel_{200}-TSC/NMMO solution and ethanol were used as a starting cellulosic material and a poor solvent for film precipitation, respectively. TSC-modification was not required for spin coating; however, the starting material of Cel_{200}-film was chemically that the same as that of Cel_{200}-SAM.

All resulting cellulosic nanolayers were dried with a flow of inert nitrogen gas and then sterilized via UV irradiation (12 h) for the cell culture assay.

2.3. Contact angle measurement

The contact angle (CA) of water droplets on the cellulosic nanolayers was measured with a DropMaster 500 (Kyowa Interface Science Co. Ltd., Japan) contact angle meter using the sessile drop technique. A water drop (1.0 μL) was gently placed on the cellulosic nanolayer at 20 °C. Digital images of the water droplets on the surfaces were periodically captured and simultaneously analyzed using the FACE analytical software (ver. 2.0.6) equipped with this apparatus.

2.4. Cell adhesion assay

The sterilized cellulosic nanolayers on gold-coated glass plates were placed on 24-well TCPS plates. IAR-20 suspensions (1 mL) were seeded on each substrate (1.0×10^5 cells mL^{-1}) and incubated for 3, 6, 12, 24, 72, and 120 h with complete EMEM medium supplemented with 10% (v/v) FBS and 5% (v/v) penicillin–streptomycin in a 5% CO_2 atmosphere at 37 °C. After the removal of unattached cells by twice rinsing with PBS, the cells were treated with trypsin–EDTA and then the detached cells were counted using a counting chamber ($n > 4$).

A cell adhesion assay using a serum-free medium was also carried out on the cellulose substrates. The pre-incubated cells were detached by trypsin–EDTA treatment and then rinsed with a fresh medium without serum by undergoing centrifugation (1500 rpm, 5 min) three times. IAR-20 (1.0×10^5 cells mL^{-1}) was seeded (1 mL) and incubated on each substrate for 3 h, and then the adhered cells were counted by the above mentioned protocol ($n > 4$).

2.5. Microscopic observation

All microscopic images were acquired with a Leica DMI 4000B (Leica Microsystems Co. Ltd., Germany). After 24 h incubation, the cell viability was optically assessed using a live/dead viability assay kit from Molecular Probes (L-3224).

3. Results and discussion

3.1. Wettability of cellulosic nanolayers

Cel_{200}-SAM evidently possesses cellulose I structure (parallel) (Yokota et al., 2007a), while Cel_{200}-film possesses cellulose II structure (anti-parallel) with lower crystallinity similar to that of common regenerated cellulose films (Eriksson, Notley, & Wågberg, 2007; Yokota et al., 2007c). In addition, the SAM-preparation method can be simply applied to water-soluble cellulose derivatives like MC (Yokota et al., 2007b) and HEC. Thus, several cellulosic interfacial materials were obtained with controlled surface morphology, which generated interest in the relationship between surface morphology and the biological function of cellulosic nanolayers. These cellulosic nanolayers are optically transparent substrates; for example, a photograph of Cel_{200}-SAMs is shown in Fig. 1. High transparency is a significant advantage in the observation of culturing cells with conventional optical microscopic apparatus, though there are almost no transparent materials in general native cellulose products such as papers and woven cotton fabrics.

The wettability of biomaterial is one of the important surface properties for cell–substrate interactions such as cell adhesion; therefore, the surface wettability of cellulosic nanolayers was investigated by the CA measurement of water droplets. Table 1 lists the values of CA on each substrate. The CA values of all cellulosic SAMs decreased from the value for the cellulose-free gold plate evidently owing to the modification of its surface with relatively hydrophilic cellulosic-TSC molecules.

The CA of a water droplet on the Cel_{200}-film was *ca.* 26° as shown in Table 1. This value incidentally agrees with those of amorphous cellulose films prepared from dimethylacetamide/lithium chloride solution (CA: 25–35°) (Eriksson et al., 2005; Sczech & Riegler, 2006). On the other hand, the cellulose film prepared from the NMMO-system by spin coating had a relatively hydrophilic surface (CA: *ca.* 17°) (Eriksson et al., 2007). X-ray photoelectron spectroscopic (XPS) analysis confirmed the surface of Cel_{200}-film had a pure cellulose-derived composition (TSC-derived sulfur and nitrogen were not detected, data not shown). Cel_{200}-film was precipitated using ethanol, while previously reported cellulose film (Eriksson et al., 2007) was precipitated using deionized water. This difference in the methods for film-preparation might affect the wettability of cellulose film surfaces.

The surface of Cel_{200}-SAM showed greater hydrophobic behavior (CA: *ca.* 42°) in comparison to the Cel_{200}-film (Table 1). It was also confirmed by XPS analysis that Cel_{200}-SAM had a pure and clean cellulose surface (Yokota et al., 2007a). The difference in the CA values might be attributed to the differences in crystallographic characteristics: Cel_{200}-SAM and Cel_{200}-film consist of cellulose I and cellulose II, respectively. The wettability of cellulosic nanolayers was probably affected by their crystallinity (Cel_{200}-film has a lower crystallinity) because of the swelling of amorphous regions of cellulose in water (Eriksson et al., 2005; Kontturi, Thüne, Alexeev, & Niemantsverdriet, 2005; Notley & Wågberg, 2005). The CA of a water droplet on the non-woven-like film with cellulose I (*ca.* 20°) (Eriksson et al., 2007) is considerably lower than that for Cel_{200}-SAM, possibly owing to the negatively charged nanocrystal surface with sulfate groups (Edgar & Gray, 2003). The Cel_6-SAM composed of water-soluble cellooligosaccharide thiosemicarbazone demonstrated more hydrophilic behavior than did Cel_{200}-SAM, indicating the chain length of cellulose SAM was a crit-

Table 1
Wettability of cell culture substrates

Substrate	Contact angle (°)
Cel_{200}-SAM	42.0 ± 5.2
Cel_6-SAM	32.9 ± 2.4
Cel_{200}-film	25.9 ± 1.8
MC-SAM	48.9 ± 1.7
HEC-SAM	41.2 ± 1.6
Gold plate	56.5 ± 5.8
TCPS	53.9 ± 2.1

ical factor in its wettability. Moreover, the surface roughness is a significant factor in wettability; hence, we will investigate the topography of cellulose nanolayers on the order of nano and micrometer scales in the near future.

Regarding cellulose derivative nanolayers, the CA values of MC- and HEC-SAMs were *ca.* 49° and *ca.* 41°, respectively (Table 1). This reasonable result was presumably due to the difference in the side-chain structures of cellulose derivatives; that is, hydrophobic methyl and hydrophilic hydroxyethyl groups probably determined the wettability.

3.2. Cell affinity for cellulose nanolayers

To investigate the interactions between IAR-20 and cellulose surfaces, a cell adhesion assay was carried out on the cellulose SAMs and film in addition to TCPS and cellulose-free gold plates as controls. Fig. 2 compares the number of cells adhered onto each substrate within 3 h of cell seeding. In the case of using the complete EMEM medium containing serum, IAR-20 significantly adhered to Cel_{200}-SAM (adhesion rate: *ca.* 40%), which is comparable to the adherence to the cellulose-free gold plate although the adherence was inferior to that for conventional TCPS (adhesion rate: *ca.* 70%). On the other hand, the cells barely adhered to Cel_{200}-film (adhesion rate: *ca.* 20%). As shown in Table 1 and Fig. 2, the cells attracted well onto the substrates with high CA values. It is well known adherent cells generally adhere more to a moderate hydrophobic substrate because cell adhesion occurs on the proteins contained in serum (*e.g.* fibronectin and vitronectin) once adsorbed to the surface of a culture substrate through hydrophobic interaction (Nakanishi et al., 2006). Thus, it is suggested the number of adhered cells on each substrate was attributed to the wetting property when a complete medium was used.

Subsequently, the cell adhesion assay was carried out using serum-free medium during the 3 h after cell seeding. As shown in Fig. 2, the number of adhered cells drastically decreased in comparison with the case for serum-added complete EMEM medium on TCPS, gold plate, and Cel_{200}-film (the rates of cell adhesion were below 20%). On the other hand, almost no influence of serum was observed on the initial cell adhesion to Cel_{200}-SAM (Fig. 2). These results imply the cell adhesion to the Cel_{200}-SAM surface is attributed to a direct attraction, possibly due to some specific interaction between IAR-20 and Cel_{200}-SAM, while the slight cell adhesion to Cel_{200}-film might occur via protein-mediated adsorption only in the case of using complete medium. As mentioned above, both the surfaces of Cel_{200}-SAM and Cel_{200}-film have pure cellulose from the view point of chemical composition. However, the crystal structures of these cellulose nanolayers are significantly different: Cel_{200}-SAM has cellulose I-type structure with parallel-chain alignment like native cellulose fibers, while Cel_{200}-film has cellulose II structure with anti-parallel alignment similar to common regenerated cellulose. The cell adhesion behavior onto Cel_6-SAM approximately agreed with that of Cel_{200}-SAM within 3 h cultivation (Fig. 2). Thus, the parallel-aligned structure of cellulose chains might play a positive role in the direct cell adhesion to surfaces of cellulose SAMs prepared by spontaneous terminal immobilization of cellulose-TSC chains.

The IAR-20 was cultured on each substrate for longer durations using complete medium (Fig. 3), and the optical and fluorescent microscopic images of cells cultured for 24 h are illustrated in Fig. 4. IAR-20 proliferated well on cellulose SAMs; in particular, the number of adhered cells on Cel_{200}-SAM exceeded that on the TCPS plate at 120 h. The majority of cells were alive on the cellulose SAMs (at 24 h, Fig. 4), indicating the cellulose SAMs had negligible cytotoxicity for IAR-20. In contrast, almost no cells proliferated on Cel_{200}-film (Fig. 3), resulting in aggregates composed of unattached and floating cells containing numerous dead cells (Fig. 4). The cell adhesion and proliferation on the regenerated film composed of unmodified cellulose (TSC-free) were approximately consistent with those of Cel_{200}-film composed of cellulose thiosemicarbazone (data not shown), strongly suggesting the TSC-component of cellulose layers (not detected in XPS spectra, data not shown) had no influence on cell adhesion and survival. In addition, excellent cell proliferation was confirmed on PVAm coated glass plate (data not shown), possibly indicating there was little cytotoxic effect caused by the elution of underlying PVAm into the culture medium. Thus, the cellulose SAMs offer the possibility of direct cell adhesion inducing a specific interaction with unique surface morphology comprising parallel-arranged molecules and also possessing a biocompatible surface property.

In previous reports, biomembranes derived from human erythrocyte ghosts were moderately immobilized on Langmuir–Blodgett cellulose film regenerated from trimethylsilyl cellulose via carbohydrate–carbohydrate interaction between cellulose and cell surface glycocalix (Tanaka, Kaufmann, Nissen, & Hochrein, 2001; Tanaka, Wong, Rehfeldt, Tutus, & Kaufmann, 2004). On the other hand, almost no rat liver cells adhered and proliferated on the Cel_{200}-film prepared from NMMO solution in this study (Figs. 2–4), probably due to differences with respect to the type of cell and its glycocalix. In other work with regard to carbohydrate-

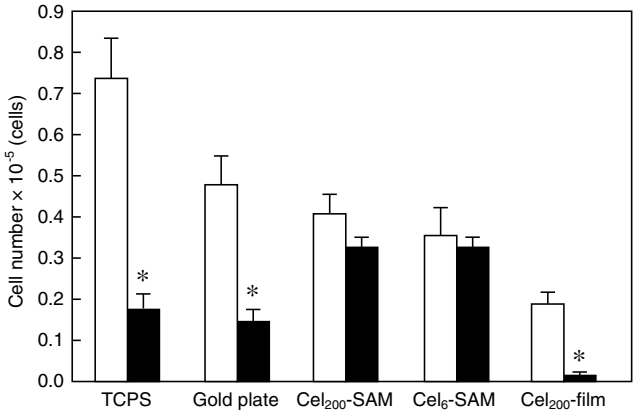

Fig. 2. Cell adhesion onto cellulose substrates after 3 h using media with (filled bars) and without serum (open bars). $^{*}p < 0.01$; serum vs. serum-free for each substrate.

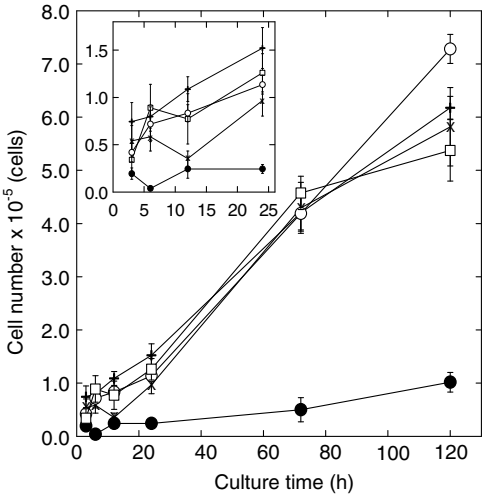

Fig. 3. Cell adhesion onto cellulose substrates at 3, 6, 12, 24, 72, and 120 h. Cel_{200}-SAM (open circles), Cel_6-SAM (open squares), Cel_{200}-film (closed circles), gold plate (crosses), and TCPS (pluses). Inset: magnified graph for the first 24 h.

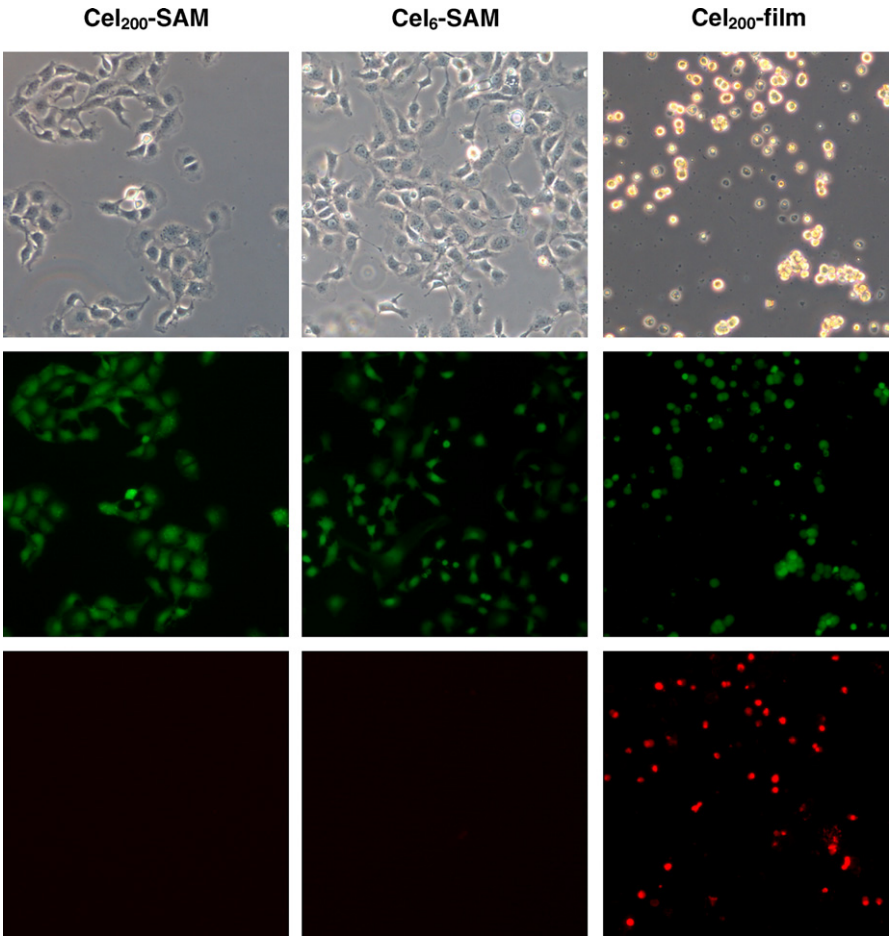

Fig. 4. Microscopic images of IAR-20 cultured on the Cel_{200}-SAM, Cel_6-SAM, and Cel_{200}-film (culture time: 24 h). (Top) Phase-contrast micrographs. (Middle and bottom) Fluorescence micrographs of live and dead cells stained with 2 μM calcein AM solution (green) and 4 μM ethidium monodimmer-1 solution (red), respectively. Image size: $500 \times 500\ \mu m^2$. (For interpretation of the references to color in this figure legend, the reader is referred to the web version of this paper.)

grafted polymers, cellooligosaccharides had significant cell (human fibroblast) adhesion properties compared with other carbohydrates (Onodera et al., 2006). Thus, the density of carbohydrate moieties at non-reducing ends on the surfaces of cellulose layers might play a key role in cell adhesion owing to carbohydrate–protein and/or carbohydrate–carbohydrate interactions. Although details of the cell adhesion mechanism between IAR-20 and cellulose SAMs remains unclear at this stage, these results are expected to open up a new phase of functional design of biointerface materials derived from cellulose-based polysaccharides.

3.3. *Effect of side-chain structure of cellulosic polymers*

Cellulosic SAMs composed of water-soluble cellulose derivatives were also successfully prepared on a gold surface via self-assembly chemisorption of their thiosemicarbazones. MC is a thermally responsive polymer such as poly(*N*-isopropylacrylamide) (Shimizu, Yamato, Kikuchi, & Okano, 2003); therefore, many researchers have studied the fundamental mechanism of the thermoresponsive sol–gel transition of MC polymers (Chevillard & Axelos, 1997; Haque & Morris, 1993) and their applications in bio and nanoengineering fields (Chen et al., 2006; Yokota et al., 2007b). Several possibilities of MC polymers as thermoresponsive substrate for cell sheet engineering have been reported (Chen et al., 2006). However, the corresponding MC films break apart easily in water at room temperature, making it difficult to apply films stably at the MC/water interface. The MC-SAM, a stable layered architecture in water, exhibited thermally responsive and reversible wetting characteristics due to the solid-state phase transition of the MC nanolayers, resulting from the inherent gelation feature of MC molecules in water (Yokota et al., 2007b). As a first step toward the application of a MC-SAM as a biofunctional interface material, the property of the MC-SAM in cell cultivation was investigated in the present study. In addition, the HEC-SAM was prepared from HEC, non-ionic cellulose derivative without a thermoresponsive gelation property, and its bioactivity investigated.

The numbers of cells adhering to MC- and HEC-SAMs with complete EMEM medium during the initial culture time (3 h after seeding) are shown in Fig. 5. The rate of cell adhesion onto the MC-SAM (*ca.* 25%) was significantly higher than that onto the HEC-SAM (*ca.* 10%). The continuous incubation undoubtedly changed the cell affinity for the MC- and HEC-SAMs as plotted in Fig. 5: the cells proliferated to eventually confluent on the MC-SAM, while almost no cell growth was observed on the HEC-SAM. These results agreed with the optical and fluorescent microscopic images (Fig. 6): numerous adhered and spread cells and huge aggregates containing dead cells were detected on MC- and HEC-SAMs, respectively.

As discussed previously, cell adhesion was generally induced by non-specific adsorption of proteins through hydrophobic interactions to moderate hydrophobic substrates (Nakanishi et al., 2006). MC-SAM had a CA value (*ca.* 49°) higher than that of HEC-SAM (*ca.* 41°) as listed in Table 1. Therefore, it is simply reasoned that the adhesion and proliferation of IAR-20 to MC-SAM are

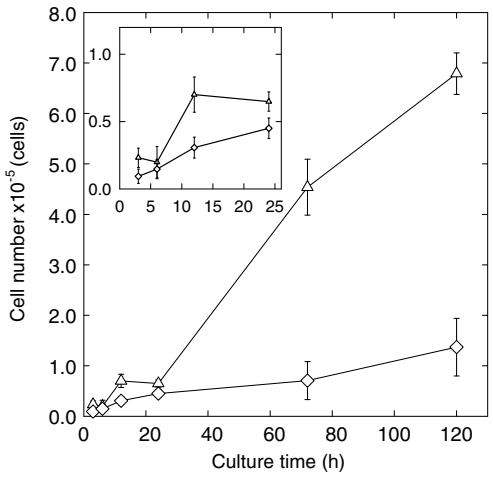

Fig. 5. Cell adhesion onto MC-SAM (open triangles) and HEC-SAM (open diamonds) at 3, 6, 12, 24, 72, and 120 h. Inset: magnified graph within 24 h.

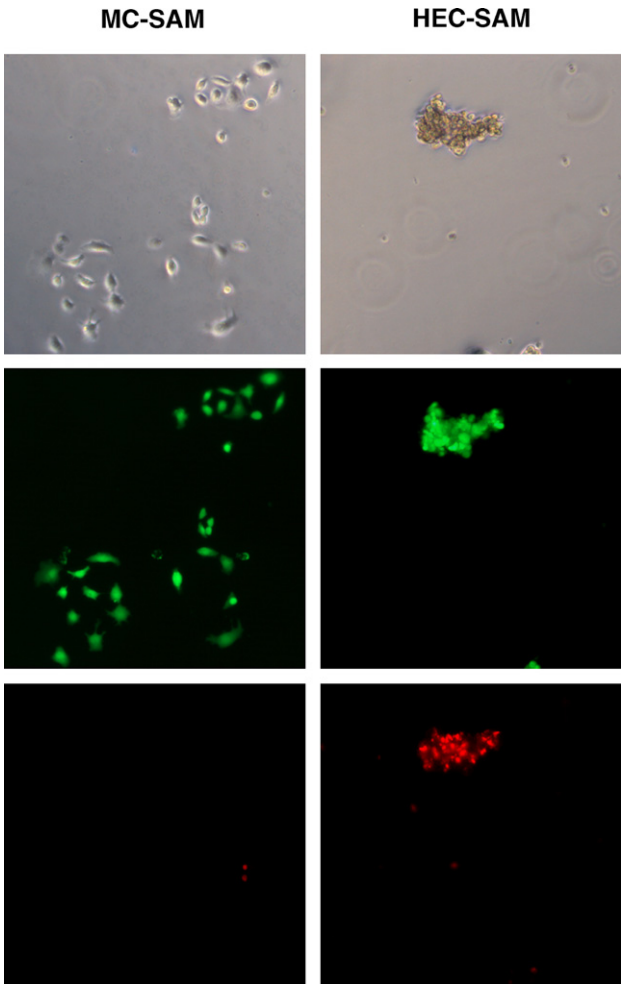

Fig. 6. Microscopic images of IAR-20 cultured on MC-SAM and HEC-SAM (culture time: 24 h). (Top) Phase-contrast micrographs. (Middle and bottom) Fluorescence micrographs of live and dead cells stained with 2 μM calcein AM solution (green) and 4 μM ethidium monodimmer-1 solution (red), respectively. Image size: 500 - 500 μm^2. (For interpretation of the references to color in this figure legend, the reader is referred to the web version of this paper.)

attributed to the hydrophobic surface of MC-SAM owing to the hydrophobic methyl groups of MC polymer. On the other hand, the HEC polymer heterogeneously has hydrophilic flexible oligo(ethylene oxide) side-chains on its backbone, suggesting the non-specific adsorption of protein was effectively prevented by the hydroxyethylated side-chains, resulting in less adhesion of IAR-20 on the HEC-SAM as for reported bioinert polymers (Ishihara, Aragaki, Ueda, Watanabe, & Nakabayashi, 1990; Zhu & Marchant, 2006). Cel_{200}- and Cel_6-SAMs had CA values the same as or lower than that of HEC-SAM possibly supporting the idea that IAR-20 was attracted to Cel-SAMs not only owing to a simple hydrophobic interaction.

Thus, the cell adhesion behavior was drastically different on MC- and HEC-SAMs constructed with reducing end-tethered polysaccharide chains. These results are expected to assist in the design of diverse functions of cellulosic SAMs for biological applications, because most polysaccharides allow the application of the vectorial chain immobilization technique.

4. Conclusion

Cellulosic nanolayers with unique surface morphology were designed by vectorial chain immobilization and self-assembling chemisorption, and their biological properties were investigated. The biocompatible cellulose SAMs stimulated moderate cell adhesion despite there being serum in the culture medium, possibly indicating some sort of specific interaction between IAR-20 and the cellulose I surface with parallel-chain alignment. Drastic regulation of the cell response was achieved for MC- and HEC-SAMs due to the property of their side-chain groups; cell adhesion was induced by hydrophobic methyl groups, while hydrophilic hydroxyethyl groups interfered with protein adsorptions and cell adhesions. Thus, the architectural design of cellulosic nanolayers via terminal chain immobilization is expected to open up a new phase in the material design of cellulose and other polysaccharide-related biofunctional interfaces.

Acknowledgments

This research was supported by a Research Fellowship from the Japan Society for the Promotion of Science for Young Scientists (S.Y.) and by a Grant-in-Aid for Young Scientists (No. 17688008) from the Ministry of Education, Culture, Sports, Science and Technology (MEXT), Japan (T.K.).

References

Atalla, R. H., & VanderHart, D. L. (1984). Native cellulose: A composite of two distinct crystalline forms. *Science, 223*, 283–285.

Bodin, A., Ahrenstedt, L., Fink, H., Brumer, H., Risberg, B., & Gatenholm, P. (2007). Modification of nanocellulose with a xyloglucan–RGD conjugate enhances adhesion and proliferation of endothelial cells: Implications for tissue engineering. *Biomacromolecules, 8*, 3697–3704.

Boyan, B. D., Hummert, T. W., Dean, D. D., & Schwartz, Z. (1996). Role of material surfaces in regulating bone and cartilage cell response. *Biomaterials, 17*, 137–146.

Chanzy, H., & Henrissat, B. (1985). Unidirectional degradation of valonia cellulose microcrystals subjected to cellulase action. *FEBS Letters, 184*, 285–288.

Chen, C.-H., Tsai, C.-C., Chen, W., Mi, F.-L., Liang, H.-F., Chen, S.-C., et al. (2006). Novel living cell sheet harvest system composed of thermoreversible methylcellulose hydrogels. *Biomacromolecules, 7*, 736–743.

Chevillard, C., & Axelos, M. A. V. (1997). Phase separation of aqueous solution of methylcellulose. *Colloid and Polymer Science, 275*, 537–545.

Couet, F., Rajan, N., & Mantovani, D. (2007). Macromolecular biomaterials for scaffold-based vascular tissue engineering. *Macromolecular Bioscience, 7*, 701–718.

Czaja, W. K., Young, D. J., Kawecki, M., & Brown, R. M. Jr., (2007). The future prospects of microbial cellulose in biomedical applications. *Biomacromolecules, 8*, 1–12.

Du, Y., Chia, S.-M., Han, R., Chang, S., Tang, H., & Yu, H. (2006). 3D hepatocyte monolayer on hybrid RGD/galactose substratum. *Biomaterials, 27*, 5669–5680.

Edgar, C. D., & Gray, D. G. (2003). Smooth model cellulose I surfaces from nanocrystal suspensions. *Cellulose, 10*, 299–306.

Eriksson, J., Malmsten, M., Tiberg, F., Callisen, T. H., Damhus, T., & Johansen, K. S. (2005). Enzymatic degradation of model cellulose films. *Journal of Colloid and Interface Science, 284*, 99–106.

Eriksson, M., Notley, S. M., & Wågberg, L. (2007). Cellulose thin films: Degree of cellulose ordering and its influence on adhesion. *Biomacromolecules, 8*, 912–919.

Haque, A., & Morris, E. R. (1993). Thermogelation of methylcellulose. Part I: Molecular structures and processes. *Carbohydrate Polymer, 22*, 161–173.

Hieta, K., Kuga, S., & Usuda, M. (1984). Electron staining of reducing ends evidences a parallel-chain structure in valonia cellulose. *Biopolymers, 23*, 1807–1810.

Hoenich, N. (2006). Cellulose for medical applications: Past, present, and future. *BioResources, 1*, 270–280.

Ishihara, K., Aragaki, R., Ueda, T., Watanabe, A., & Nakabayashi, N. (1990). Reduced thrombogenicity of polymers having phospholipid polar groups. *Journal of Biomedical Materials Research, 24*, 1069–1077.

Isogai, A., & Usuda, M. (1991). Preparation of low-molecular-weight celluloses using phosphoric-acid. *Mokuzai Gakkaishi, 37*, 339–344.

Jagur-Grodzinski, J. (2006). Polymers for tissue engineering, medical devices, and regenerative medicine. Concise general review of recent studies. *Polymers for Advanced Technologies, 17*, 395–418.

Klemm, D., Schumann, D., Udhardt, U., & Marsch, S. (2001). Bacterial synthesized cellulose – Artificial blood vessels for microsurgery. *Progress in Polymer Science, 26*, 1561–1603.

Klemm, D., Heublein, B., Fink, H.-P., & Bohn, A. (2005). Cellulose: Fascinating biopolymer and sustainable raw material. *Angewandte Chemie, International Edition, 44*, 3358–3393.

Klemm, D., Schumann, D., Kramer, F., Hessler, N., Hornung, M., Schmauder, H.-P., et al. (2006). Nanocelluloses as innovative polymers in research and application. *Advances in Polymer Science, 205*, 49–96.

Kolpak, F. J., & Blackwell, J. (1976). Determination of the structure of cellulose II. *Macromolecules, 9*, 273–278.

Kontturi, E., Thüne, P. C., Alexeev, A., & Niemantsverdriet, J. W. (2005). Introducing open films of nanosized cellulose – Atomic force microscopy and quantification of morphology. *Polymer, 46*, 3307–3317.

Kontturi, E., Tammelin, T., & Österberg, M. (2006). Cellulose-model films and the fundamental approach. *Chemical Society Reviews, 35*, 1287–1304.

Langan, P., Nishiyama, Y., & Chanzy, H. (1999). A revised structure and hydrogen-bonding system in cellulose II from a neutron fiber diffraction analysis. *Journal of the American Chemical Society, 121*, 9940–9946.

Lim, J. Y., Liu, X., Vogler, E. A., & Donahue, H. J. (2004). Systematic variation in osteoblast adhesion and phenotype with substratum surface characteristics. *Journal of Biomedical Materials Research A, 68*, 504–512.

Lim, J. Y., Dreiss, A. D., Zhou, Z., Hansen, J. C., Siedlecki, C. A., Hengstebeck, R. W., et al. (2007). The regulation of integrin-mediated osteoblast focal adhesion and focal adhesion kinase expression by nanoscale topography. *Biomaterials, 28*, 1787–1797.

Nakanishi, J., Kikuchi, Y., Takarada, T., Nakayama, H., Yamaguchi, K., & Maeda, M. (2006). Spatiotemporal control of cell adhesion on a self-assembled monolayer having a photocleavable protecting group. *Analytica Chimica Acta, 578*, 100–104.

Nishio, Y. (2006). Material functionalization of cellulose and related polysaccharides via diverse microcompositions. *Advances in Polymer Science, 205*, 97–151.

Nishiyama, Y., Langan, P., & Chanzy, H. (2002). Crystal structure and hydrogen-bonding system in cellulose I_β from synchrotron X-ray and neutron fiber diffraction. *Journal of the American Chemical Society, 124*, 9074–9082.

Nishiyama, Y., Sugiyama, J., Chanzy, H., & Langan, P. (2003). Crystal structure and hydrogen bonding system in cellulose I_α from synchrotron X-ray and neutron fiber diffraction. *Journal of the American Chemical Society, 125*, 14300–14306.

Notley, S. M., & Wågberg, L. (2005). Morphology of modified regenerated model cellulose II surfaces studied by atomic force microscopy: Effect of carboxymethylation and heat treatment. *Biomacromolecules, 6*, 1586–1591.

Onodera, T., Niikura, K., Iwasaki, N., Nagahori, N., Shimaoka, H., Kamitani, R., et al. (2006). Specific cell behavior of human fibroblast onto carbohydrate surface detected by glycoblotting films. *Biomacromolecules, 7*, 2949–2955.

Park, I.-K., Yang, J., Jeong, H.-J., Bom, H.-S., Harada, I., Akaike, T., et al. (2003). Galactosylated chitosan as a synthetic extracellular matrix for hepatocytes attachment. *Biomaterials, 24*, 2331–2337.

Schenzel, K., & Fischer, S. (2001). NIR FT Raman spectroscopy – A rapid analytical tool for detecting the transformation of cellulose polymorphs. *Cellulose, 8*, 49–57.

Sczech, R., & Riegler, H. (2006). Molecularly smooth cellulose surfaces for adhesion studies. *Journal of Colloid and Interface Science, 301*, 376–385.

Shimizu, T., Yamato, M., Kikuchi, A., & Okano, T. (2003). Cell sheet engineering for myocardial tissue reconstruction. *Biomaterials, 24*, 2309–2316.

Svensson, A., Nicklasson, E., Harrah, T., Panilaitis, B., Kaplan, D. L., Brittberg, M., et al. (2005). Bacterial cellulose as a potential scaffold for tissue engineering of cartilage. *Biomaterials, 26*, 419–431.

Tanaka, M., Kaufmann, S., Nissen, J., & Hochrein, M. (2001). Orientation selective immobilization of human erythrocyte membranes on ultrathin cellulose films. *Physical Chemistry Chemical Physics, 3*, 4091–4095.

Tanaka, M., Wong, A. P., Rehfeldt, F., Tutus, M., & Kaufmann, S. (2004). Selective deposition of native cell membranes on biocompatible micropatterns. *Journal of the American Chemical Society, 126*, 3257–3260.

Wang, F., & Tanaka, H. (2000). Aminated poly-*N*-vinylformamide as a modern retention aid of alkaline paper sizing with acid rosin sizes. *Journal of Applied Polymer Science, 78*, 1805–1810.

Yokota, S., Kitaoka, T., Sugiyama, J., & Wariishi, H. (2007a). Cellulose I nanolayers designed by self-assembly of its thiosemicarbazone on a gold substrate. *Advanced Materials, 19*, 3368–3370.

Yokota, S., Matsuyama, K., Kitaoka, T., & Wariishi, H. (2007b). Thermally responsive wettability of self-assembled methylcellulose nanolayers. *Applied Surface Science, 253*, 5149–5154.

Yokota, S., Kitaoka, T., & Wariishi, H. (2007c). Surface morphology of cellulose films prepared by spin coating on silicon oxide substrates pretreated with cationic polyelectrolyte. *Applied Surface Science, 253*, 4208–4214.

Zhu, J., & Marchant, R. E. (2006). Dendritic saccharide surfactant polymers as antifouling interface materials to reduce platelet adhesion. *Biomacromolecules, 7*, 1036–1041.